International Journal of Nanomedicine

Dovepress
open access to scientific and medical research

Open Access Full Text Article

ORIGINAL RESEARCH

Magnetite Fe_3O_4 Nanoparticles Enhance Mild Microwave Ablation of Tumor by Activating the IRE1-ASK1-JNK Pathway and Inducing Endoplasmic Reticulum Stress

Shuai Li[1,*]
Yi Liu[1,*]
Xinyi Liu[2,*]
Bin Lan[1]
Wanwan Li[1,2]
Fang Guo[1]

[1]Key Laboratory of Systems Biomedicine (Ministry of Education), Shanghai Center for Systems Biomedicine, Shanghai Jiao Tong University, Shanghai, 200240, People's Republic of China; [2]State Key Laboratory of Metal Matrix Composites, School of Materials Science and Engineering, Shanghai Jiao Tong University, Shanghai, 200240, People's Republic of China

*These authors contributed equally to this work

Purpose: With the development of nanomedicine, microwave ablation enhanced by multifunctional nanoplatforms has been widely studied for synergistic cancer therapy. Though scientists have got a lot of significant achievements in this field, the detailed molecular mechanisms and potential targets of microwave ablation enhanced by multifunctional nanoplatforms still need further exploration. In this study, we found that a kind of magnetite Fe_3O_4 nanoparticles (Fe_3O_4 NPs) could induce severe endoplasmic reticulum stress and activate cancer apoptosis under the irradiation of mild microwave.

Methods: In this study, plenty of studies including cell immunofluorescence, mitochondrial membrane potential, electron microscopy, atomic force microscopy and microwave ablation in vivo were conducted to explore the molecular mechanisms and potential targets of microwave ablation enhanced by the Fe_3O_4 NPs.

Results: The IRE1-ASK1-JNK pathway was strongly activated in A375 cells treated with both Fe_3O_4 NPs and mild microwave. The endoplasmic reticulum of the A375 cells was significantly dilated and exhibited ballooning degeneration. By investigating the mitochondrial membrane potential ($\Delta\Psi m$), we found that the mitochondria of cancer cells had been significantly damaged under microwave treatment coupled with Fe_3O_4 NPs. In addition, melanoma of B16F10-bearing mice had also been effectively inhibited after being treated with Fe_3O_4 NPs and microwave.

Conclusion: In this study, we found that a kind of magnetite Fe_3O_4 nanoparticles could induce severe ER stress and activate cancer apoptosis under mild microwave irradiation. Apparent apoptosis had been observed in the A375 cells under a scanning electron microscope and transmission electron microscope. Moreover, melanoma had also been inhibited effectively in vivo. As a result, the endoplasmic reticulum stress is a promising target with clinical potential in nanomedicine and cancer therapy.

Keywords: microwave ablation, ER stress, apoptosis, magnetite Fe_3O_4 nanoparticles

Correspondence: Wanwan Li
State Key Laboratory of Metal Matrix Composites, School of Materials Science and Engineering, Shanghai Jiao Tong University, 800 Dongchuan Road, Shanghai, 200240, People's Republic of China
Email wwli@sjtu.edu.cn

Fang Guo
Key Laboratory of Systems Biomedicine (Ministry of Education), Shanghai Center for Systems Biomedicine, Shanghai Jiao Tong University, 800 Dongchuan Road, Shanghai, 200240, People's Republic of China
Email fguo@sjtu.edu.cn

Introduction

In recent years, biomaterials are in the spotlight.[1] Microwave ablation enhanced by multifunctional nanoplatforms has been widely studied for synergistic cancer therapy. For instance, in Long's study, multifunctional nanoplatforms have been designed for enhanced tumor microwave ablation by loading phase change materials (PCMs), doxorubicin hydrochloride (DOX), and ionic liquids (ILs) into ZrO_2

Received: 25 March 2021
Accepted: 29 July 2021
Published: 3 September 2021

hollow nanoparticles.[2] However, the detailed molecular mechanisms and potential targets of microwave ablation enhanced by multifunctional nanoplatforms still need further exploration.

The endoplasmic reticulum (ER) is a network of flattened sacs and branching tubules that governs the processing, folding, and synthesis of over a third of all cellular proteins. Many conditions that impose stress on cells, including starvation, hypoxia, loss of calcium homeostasis, and so on, promote ER stress.[3–6] To restore homeostasis, the cellular response involves the activation of sensors transducing signaling cascades. This is known as the unfolded protein response (UPR). Central to the UPR are the sensors activating transcription factor 6 (ATF6), protein kinase RNA-activated (PKR)-like ER kinase (PERK), and inositol requiring enzyme 1 (IRE1). Of which, IRE1 activates the most conserved UPR signaling branch. If the severe ER stress cannot be attenuated or the homeostasis cannot be restored, terminal UPR will be triggered, which leads to apoptosis. As a result, ER stress is a potential target for cancer therapy.[7]

In this study, we found that a kind of magnetite Fe_3O_4 nanoparticles (Fe_3O_4 NPs) could induce severe ER stress and activate cancer apoptosis under mild microwave irradiation (Scheme 1).[8] The IRE1-ASK1-JNK pathway was strongly activated in A375 cells treated with both Fe_3O_4 NPs and mild microwave. The ER of those cells was significantly dilated and exhibited ballooning degeneration due to severe stress. Severe ER stress finally induces terminal UPR which triggers intrinsic apoptosis. Through scanning electron microscope, transmission electron microscope, and atomic force microscope, the dynamic membrane changes of apoptosis of the A375 cells were captured. After being exposed to Fe_3O_4 NPs and microwave for 20 min, wrinkled cells covered with membrane blebbing and apoptotic body were found, indicating apoptosis had been fully activated. Moreover, mitochondria play an important role in intrinsic apoptosis. Apoptosis will be activated when the mitochondrial membrane is damaged and then cytochrome c is released into the cytosol. In this study, by investigating the mitochondrial membrane potential ($\Delta\Psi m$), we found that the mitochondria of cancer cells had been significantly damaged under microwave treatment coupled with Fe_3O_4 NPs. Meanwhile, under the TEM, we also observed the disappearance of mitochondrial cristae and abnormal mitochondrial membrane swelling and rupture. In addition, melanoma of B16F10-bearing mice had also been effectively inhibited after being treated with Fe_3O_4 NPs and microwave. Owing to the mild microwave, the treatment in this study may cause less damage to normal tissues adjacent to cancer. In summary, our results demonstrate that ER stress is a promising target with clinical potential in nanomedicine and cancer therapy.

Experimental Section

Materials

Tri-sodium citrate dihydrate was bought from Sigma-Aldrich (Shanghai) Trading Co. Ltd. (Shanghai, China). $FeCl_3 \cdot 6H_2O$ was obtained from the Instrumental Analysis Center of Shanghai Jiao Tong University (Shanghai, China). Phospho-ASK1 (Thr838) antibody (AF8096) was obtained from Affinity (Cincinnati, OH, USA). Anti-IRE1 (phosphor S724) antibody (ab48187) and Anti-JNK1 (phosphor T183 + Y185) antibody were obtained from Abcam (Cambridge, MA, USA). DAPI was bought from Roche. Neutral resin, osmic acid, and glutaraldehyde were obtained from the Instrumental Analysis Center of Shanghai Jiao Tong University. A375 cells and B16F10 cells were obtained from the Key Laboratory of Systems Biomedicine (Ministry of Education). C57BL/6 mice were bought from the Laboratory Animal Center of Shanghai Jiao Tong University. Mitochondrial membrane potential assay kit with JC-1 was bought from Beyotime (Shanghai, China).

Cell Immunofluorescence

A375 cells were treated with PBS, microwave, Fe_3O_4, or Fe_3O_4 + microwave, respectively. The microwave irradiation time is 10 min (2450 MHz, 2 W) and the concentration of Fe_3O_4 is 30 μg/mL. The treated A375 cells in each group were fixed with 4% paraformaldehyde for 30 min at room temperature and then incubated in 0.1% PBS-Tween for 8 min to permeabilise the cells. Then, the cells were incubated in 10% BSA for 1 h. The cells then were incubated with primary antibody overnight at 4 °C. Then the cells were incubated with secondary antibody for 2 h at room temperature. DAPI was used to stain the cell nuclei. A confocal laser scanning microscope (Nikon, A1Si) was used to observe the cells.

Mitochondrial Membrane Potential

JC-1 assay was used to measure the mitochondrial membrane potential of cells in each group. The treated cells were incubated with JC-1 for 20 min at 37 °C, and then

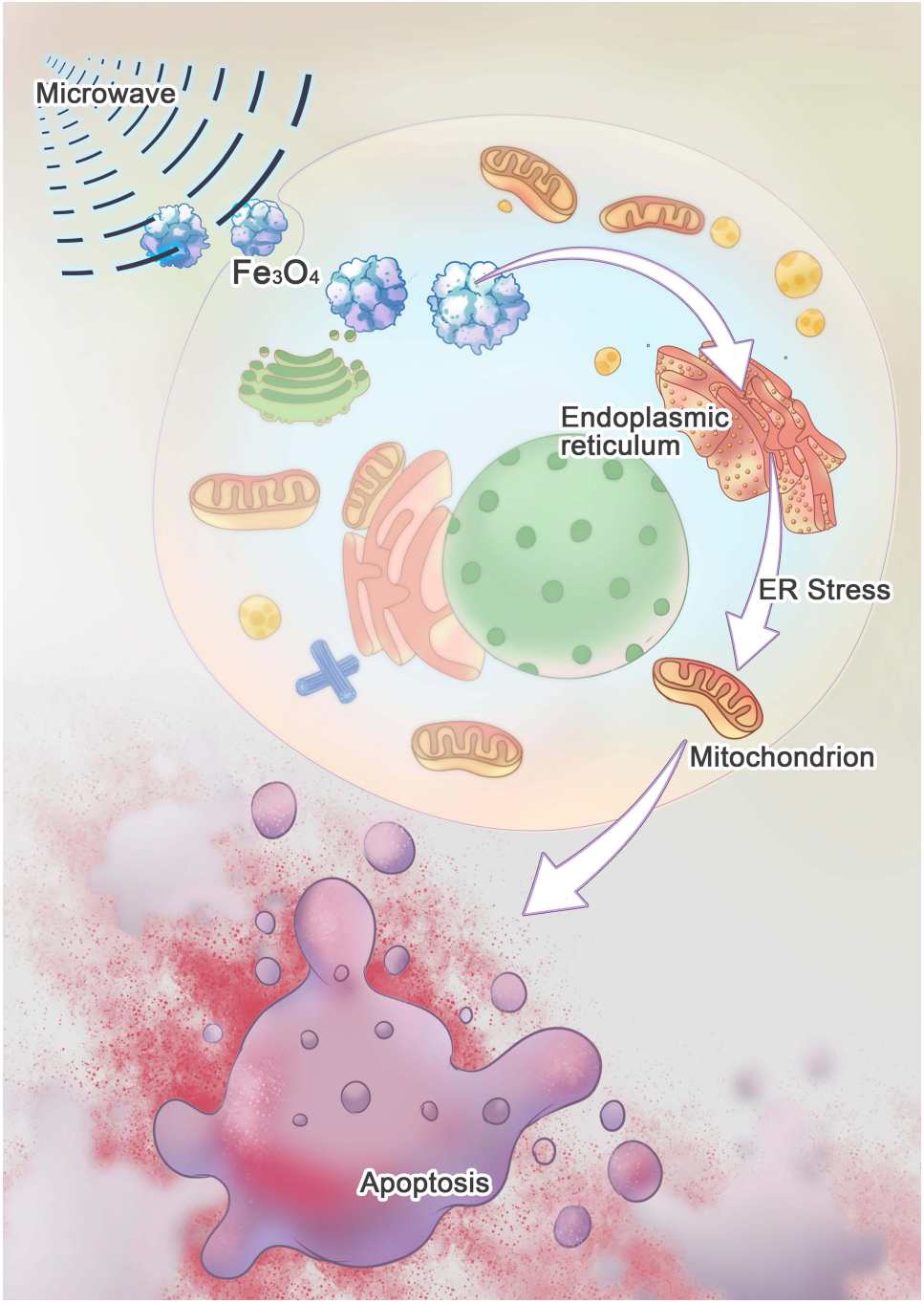

Scheme 1 Fe_3O_4 nanoparticles could induce severe endoplasmic reticulum stress and activate cancer apoptosis under the irradiation of mild microwave.

washed with PBS. DAPI was used to stain the cell nuclei. The cells were observed under a confocal laser scanning microscope (Nikon, A1Si).

Cell Culture

Human melanoma cell-line A375 was cultured in DMEM medium in a 5% CO_2 humidified atmosphere at 37 °C. The medium was supplemented with 10% FBS (Gibco).

Electron Microscopy

For TEM, cells were fixed with 2.5% glutaraldehyde, rinsed with PBS, postfixed in 1% osmium tetroxide, dehydrated through a graded series of ethanol (50–90%), and embedded in resin for 48 h at 60 °C. Ultrathin sections were observed under a transmission electron microscope (Thermo Scientific, Talos L120C G2).

For SEM, cells were fixed with 2.5% glutaraldehyde and dehydrated through a graded series of ethanol (50–100%). Then, the cells were dried in a critical point dryer (Leica, EM CPD300). The cells were observed under a Raman imaging combined with emission scanning electron microscope (TESCAN, MAIA3 GMU).

Atomic Force Microscopy

A375 cells treated with Fe_3O_4 were irradiated by microwave (2450 MHz, 2 W) for different time periods (5, 10, 15, and 20 min). Then, the cells were fixed with 2.5% glutaraldehyde and observed by an atomic force microscope (BRUKER, FastScan).

Microwave Ablation in vivo

Six- to eight-week-old female C57BL/6 mice were raised with free access to food and water. Tumor models were established by subcutaneously injecting 5.0×10^5 B16F10 cells into C57BL/6 mice. B16F10 tumor-bearing mice (tumor size in any direction not exceeding 10 mm) were randomly divided into the following three treatment groups: PBS, microwave, and Fe_3O_4 + microwave. The Fe_3O_4 NPs were injected into the mice via the tail vein, and injection dose was 50 mg/Kg. Twelve-hour post-injection, the mice in the microwave and microwave + Fe_3O_4 group were irradiated by means of a microwave antenna for 25 min (4 W, 2450 MHz). The body weight and tumor size were recorded daily. The representative tumors of mice in each group were recorded by a multi-mode ultrasound imaging system (Fujifilm VisualSonics, VEVO LAZR-X) on day 0, day 6 and day 12. The tumors were reconstructed in three dimensions. On day 12, the distribution of blood vessels in tumors was observed by the multi-mode ultrasound imaging system (Fujifilm VisualSonics, VEVO LAZR-X). All animal experiments were governed by the Regulations of Experimental Animals of Shanghai Jiao Tong University (ethics approval number: 202004034, granted by Shanghai Jiao Tong University).

Synthesis of Magnetite Fe_3O_4 Particles

Tri-sodium citrate dihydrate (0.20 g) and $FeCl_3\cdot6H_2O$ (1.08 g) were dissolved in ethylene glycol (20 mL); then, NaAc (1.20 g) was added with stirring. The mixture was sealed in an autoclave after being stirred for 60 min. The autoclave was heated at 200 °C for 10 h and then allowed to cool to room temperature. The products were washed with water for 5 times.

Statistical Analysis

The statistical significance for all tests was set at $^*p < 0.05$. All results were expressed as the mean±S.D.

Results and Discussion

Characteristics of Fe_3O_4 NPs

Through the scanning electron microscopy, we find that the Fe_3O_4 NPs obtained have a nearly spherical shape (Figure 1A and B). The surface of the Fe_3O_4 NPs is uneven. Owing to the uneven surface, the Fe_3O_4 NPs may enhance the ion confinement, enhancing the effect of the mild microwave.[9–11] The diameter of the particles mainly ranges from 130 nm to 200 nm, which helps them target the tumor tissue through enhanced permeability and retention effect (EPR effect).[12,13] A TEM image shows that the nanoparticles are loose clusters (Figure 1C). The magnetization saturation value (Ms) of the Fe_3O_4 NPs is 74.7 emu/g (Figure 1D). The intense magnetism may interfere with the ion homeostasis of ER in cancer cells, resulting in ER stress.

In vivo Acute Toxicity Evaluation

It is crucial that the Fe_3O_4 NPs should not interfere with normal cells. Consequently, HE staining assay and transmission electron microscopy were used to investigate the biosafety of the Fe_3O_4 NPs. As shown in Figure 1E and F, histological sections and TEM images of major organs of mice (heart, liver, spleen, lung, and kidney) exhibit no significant abnormities. For instance, the syncytial arrangement of the fibers and intercalated disc can be found in myocardial cells. In this study, ER is the main targeted organelle. As a result, transmission electron microscopy was used to further explore nanomaterials' effect on ER in normal tissue cells. The ER of major organs (heart, liver, spleen, lung, and kidney) exhibited parallel stacked arrangement, with ribosomes covering the exterior surface. These findings indicate that the ER of normal tissue can tolerate the stimuli from the Fe_3O_4 NPs. Different from the highly proliferative state of tumor, the proliferation of normal tissue is stable. Accordingly, compared to the tumor, the load of ER of the normal tissue was much lower.[14,15] As a result, the ER in normal tissue may tolerate the mild stimuli from the Fe_3O_4 NPs. In conclusion, the Fe_3O_4 NPs in this study exhibit good biocompatibility.

The Activation of the IRE1-ASK1-JNK Pathway

The ER is a network of flattened sacs and branching tubules that governs the processing, folding, and synthesis of over

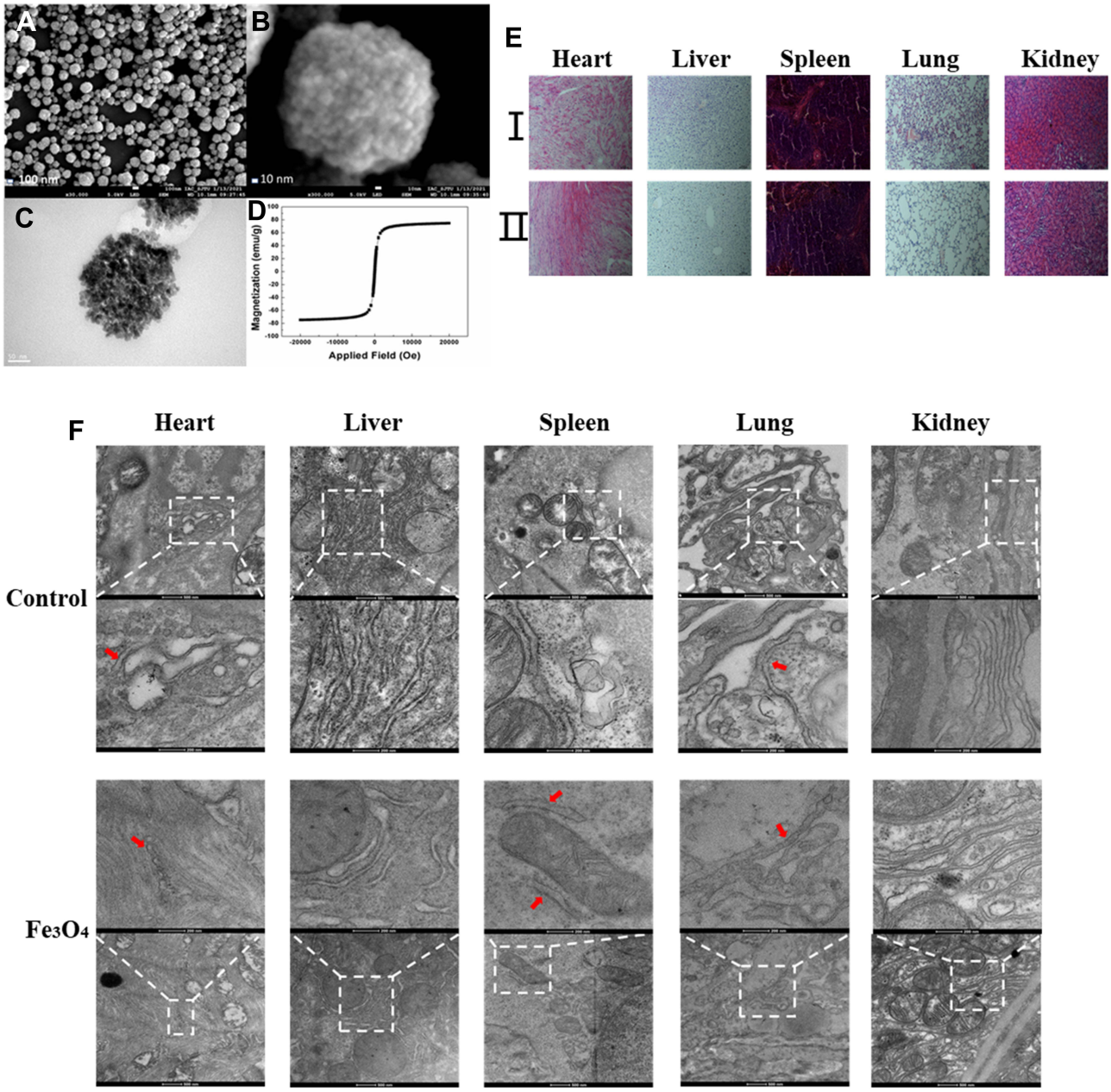

Figure 1 (**A** and **B**) Fe_3O_4 NPs imaged by SEM. (**C**) Fe_3O_4 NPs imaged by TEM. (**D**) Magnetization value of the Fe_3O_4 NPs. (**E** and **F**) In vivo acute toxicity evaluation of the Fe_3O_4 NPs (100 mg/Kg, tail vein injection, 72 h). I: control group. II: Fe_3O_4 group. The red arrows indicate endoplasmic reticulum.

a third of all cellular proteins.[15] Many conditions that impose stress on cells, including starvation, hypoxia, loss of calcium homeostasis, changes in secretory needs and so on, promote ER stress. The cellular response involves the activation of sensors transducing signaling cascades aiming to restore homeostasis. This is known as the unfolded protein response (UPR). Central to the UPR are the sensors activating transcription factor 6 (ATF6), protein kinase RNA-activated (PKR)-like ER kinase (PERK), and inositol requiring enzyme 1 (IRE1). Of which, IRE1 activates the most conserved UPR signaling branch.[3] In Huo's study, they found that silver nanoparticles can activate the IRE1 signaling pathway in cell and mouse models.[16] IRE1 activates ASK1 and its downstream protein JNK, and JNK can induce intrinsic apoptosis by inhibiting Bcl-2.[17,18] As a result, we used immunofluorescence to investigate the activation of the IRE1-ASK1-JNK pathway in A375 cells treated with Fe_3O_4 and microwave. As shown in Figure 2A, the IRE1-

ASK1-JNK pathway in the control group is hardly activated. However, weak fluorescence was found in the Fe_3O_4 group (Figure 2A), indicating that the IRE1-ASK1-JNK pathway had been slightly activated. Because cancer cells suffer more unfavorable factors than normal cells and are highly proliferating, their ER is more vulnerable.[3,4,6] Consequently, the ER may be a potential target for cancer therapy. In Yang's study, cuprous oxide nanoparticles disrupt copper transportation via regulating the copper chaperone proteins ATOX1 and CCS in renal cell carcinoma cells and induce ER stress.[19] As a result, the ER of A375 cells may be interfered by nanomaterials, and the UPR had been slightly activated. In the microwave group (Figure 2A), relatively strong fluorescence was observed. This suggests that the IRE1-ASK1-JNK pathway had been activated. In Long's study, they found that biomembranes could act as oscillating electric dipoles under microwave irradiation. The microwave passing through the membrane will lead to electronic vibrations and polarization.[2] The ER is formed by the folding of the biomembrane and may also be disturbed by the wave. As a result, the activation of the IRE1-ASK1-JNK pathway may be attributed to that the microwave interfered with the ER and protein folding. As we expected, in the Fe_3O_4 and microwave group (Figure 2A), we can find strong fluorescence. This indicates that the IRE1-ASK1-JNK pathway had been strongly activated. This may be attributed to the synergistic effect of the Fe_3O_4 NPs and microwave. The persistent microwave stimuli and interference of nanoparticles induced severe ER stress. It was hard for the ER to restore homeostasis, so the UPR was strongly activated. Since the severe ER stress could not be attenuated, terminal UPR was triggered and led to apoptosis.

Morphological Changes of Endoplasmic Reticulum

With the activation of the IRE1-ASK1-JNK pathway, the morphology of ER will be changed accordingly.[20,21] TEM was used to observe morphological changes of the ER. As shown in Figure 2B, the regular ER in normal A375 cells exhibit parallel stacked arrangement, with ribosomes covering the exterior surface. Interestingly, the ER in Fe_3O_4 group exhibits slightly dilated but there are still ribosomes covering the exterior surface (Figure 2B). It is known that the metabolic state of cancer cells is highly proliferating in an acidotic and hypoxic microenvironment. In addition to the unfavorable factors, the highly proliferative properties of cancer cells may activate the UPR response to allow cancer cells to continue to grow in nutrient-deficient environments.[22–24] As a result, the ER of cancer cells is more vulnerable than that of normal cells. Therefore, the ER of A375 cells may be interfered by the nanomaterials, and it is slightly dilated. However, the structure of ER is still relatively intact and there are still ribosomes covering the exterior surface, indicating ER is slightly damaged. It is also consistent with the results of immunofluorescence. As shown in Figure 2B, the ER of A375 cells treated with microwave are dilated, with partial remaining normal part. In addition, there are no ribosomes covering the exterior surface. These results indicate that persistent microwave stimuli can induce relatively intense ER stress. This may be due to the interference of persistent microwave on protein folding in cancer cells. The uncontrolled, rapid growth of cancer cells requires high-protein production rates, which results in a consequent impact on ER systems. With the continuous stimulation of microwave, the level of ER stress is much higher than normal conditions. Also, the biomembrane of ER may be disturbed by the microwave. As a result, the UPR is activated and the ER exhibits obviously dilated. As we expected, the ER of cells treated with both Fe_3O_4 and microwave exhibit significant abnormity (Figure 2B). The ER is significantly dilated and exhibits ballooning degeneration. In addition, parallel stacked arrangement and ribosomes have disappeared completely. Since the IRE1-ASK1-JNK pathway has been strongly activated, these results may be attributed to the severe ER stress. The lotus-like structure of the nanoparticles enhances the effect of the microwave, inducing severe ER stress. Persistent microwave stimuli and Fe_3O_4 may seriously interfere with the biomembrane and protein folding, resulting in terminal UPR.

Changes in Nuclear and Mitochondrial Membrane Potential

Severe ER stress can induce terminal UPR which triggers intrinsic apoptosis. Apoptosis is type I programmed cell death which does not induce inflammation. As a result, it is a mild type of cell death. Apoptosis is characterized by specific biochemical and morphological changes of dying cells, including nuclear condensation and fragmentation, loss of adhesion to neighbors, dynamic membrane blebbing, and so on.[25–27] Immunofluorescence confocal microscope was used to observe the morphology of the nucleus of A375 cells in different groups. As shown in Figure 2C, normal A375 cells' nuclear structure is regular and well-distributed chromoplasm can be observed. In the Fe_3O_4 group (Figure 2C), there are no noticeable abnormalities on the nucleus of A375 cells. As the

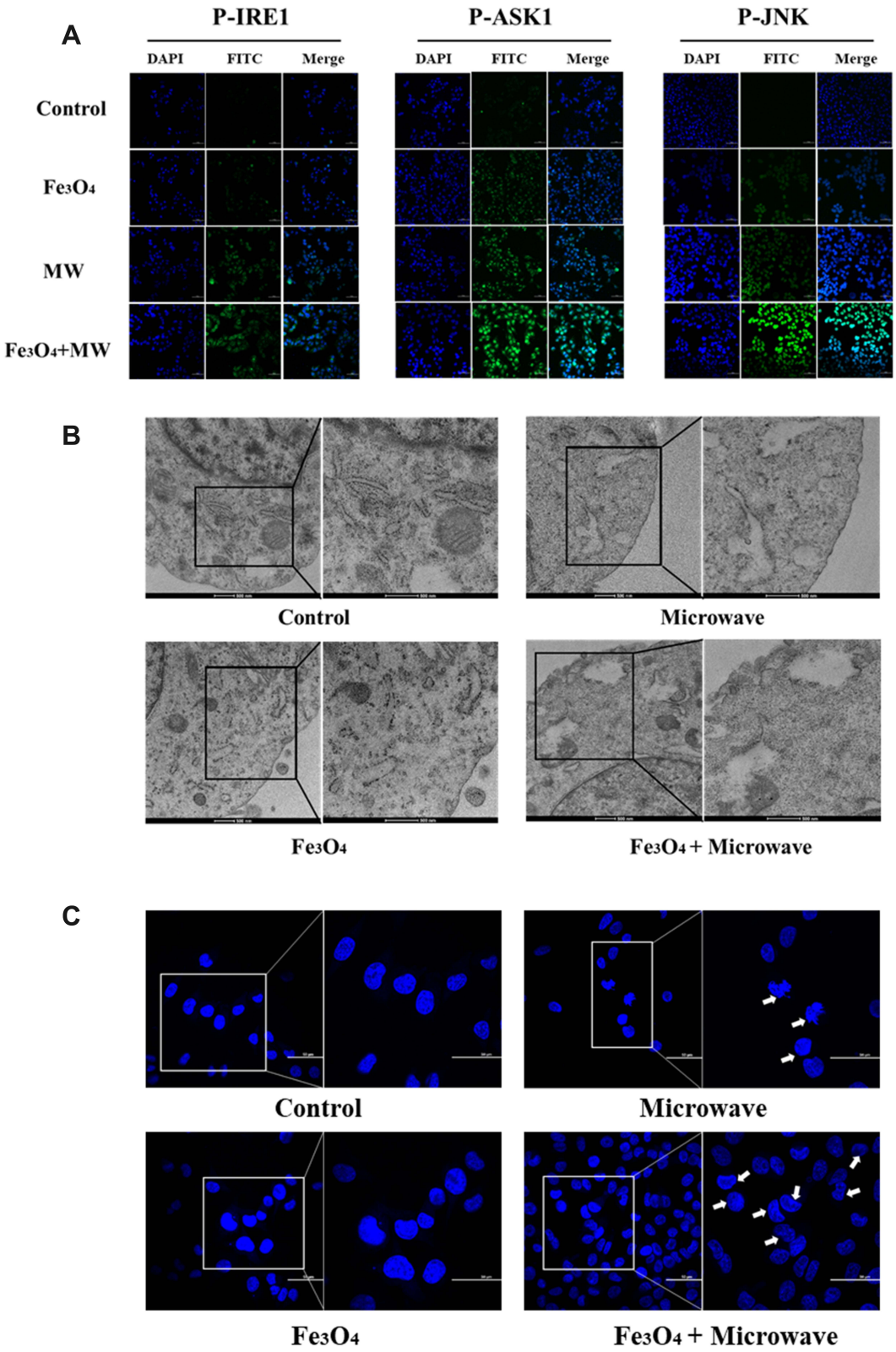

Figure 2 (**A**) Immunofluorescence images of the IRE1-ASK1-JNK pathway. The microwave (MW) irradiation time is 10 min (2450 MHz, 2W) and the concentration of Fe_3O_4 NPs is 30 μg/mL. (**B**) Morphological changes of endoplasmic reticulum. The microwave irradiation time is 10 min (2450 MHz, 2W) and the concentration of Fe_3O_4 NPs is 30 μg/mL. (**C**) Morphological changes of nuclear. The microwave irradiation time is 15 min (2450 MHz, 2W) and the concentration of Fe_3O_4 NPs is 30 μg/mL.

IRE1-ASK1-JNK pathway in the Fe_3O_4 group has not been fully activated, it is hard to trigger intrinsic apoptosis. Thus, it is difficult to find apparent abnormalities on the nuclear of A375 cells in the Fe_3O_4 group. In the microwave group (Figure 2C), we can observe obvious nuclear condensation and fragmentation. This may be attributed to that microwave induces relatively intense ER stress that activates the IRE1-ASK1-JNK pathway, triggering intrinsic apoptosis. Combined with TEM observation, we conclude that mild microwave may cause the ER to dilate by promoting ER stress. In the Fe_3O_4 + microwave group (Figure 2C), significant nuclear condensation and fragmentation can be observed. Condensed chromatin can be found around the nucleus. These findings indicate that apoptosis has been activated.[25] As shown previously, the synergistic effect of Fe_3O_4 and microwave can induce severe ER stress and strongly activate the IRE1-ASK1-JNK pathway. Consequently, significant apoptosis was triggered by the terminal UPR. As we know, the activation of the IRE1-ASK1-JNK pathway can inhibit Bcl-2 which plays an antiapoptotic role. Consequently, outer mitochondrial membranes become permeable to internal cytochrome c which is then released into the cytosol, culminating in apoptosis.[25] As a result, a principal incentive for apoptosis is mitochondrial damage.[28] The decrease of the mitochondrial membrane potential ($\Delta\Psi m$) can reflect the damage to mitochondria. In Wang's study, they found that the $\Delta\Psi m$ of HCT116 and HT29 cells treated with ch282-5 decreased significantly, which is attributed to ch282-5 binding to the BH3 domain of the Bcl-2 family antiapoptotic proteins.[28] To further explore the mechanism of microwave and Fe_3O_4 induced apoptosis, the mitochondrial-specific dual-fluorescence probe JC-1 was employed. In normal cancer cells with high $\Delta\Psi m$, JC-1 forms complexes known as J-aggregates. While in cells with low $\Delta\Psi m$, JC-1 remains in the monomeric form. Laser confocal microscope can be used to tell the different forms of JC-1. In the control group (Figure 3A), red fluorescence (J-aggregates) suggests the high $\Delta\Psi m$. In the microwave group (Figure 3A), both red fluorescence (J-aggregates) and green fluorescence (J-monomer) can be observed, indicating the mitochondria of the cells treated with microwave have been damaged. This may be attributed to that the microwave induces relatively intense ER stress that activates the IRE1-ASK1-JNK pathway, triggering apoptosis. In the Fe_3O_4 + microwave group (Figure 3A), only green fluorescence (J-monomer) can be observed, suggesting that mitochondrial has been significantly damaged under the microwave treatment coupled with Fe_3O_4. Combined with prior results, these findings of mitochondrial membrane potential further indicate that microwave coupled with Fe_3O_4 can induce apoptosis through the mitochondrial pathway by promoting severe and irreversible ER stress.

Dynamic Membrane Blebbing and Apoptotic Bodies

Apoptosis is a dynamic biological process. Dynamic membrane blebbing is one of the essential characteristics of apoptosis.[25–27] In this study, SEM and atomic force microscope (AFM) was used to capture the dynamic membrane changes of apoptosis of the A375 cells (Figure 3B). The normal A375 cells are rounded and plump with uniform villi on their surface. Under the atomic force microscope, normal A375 cells with uneven surface adhere well to the wall and pseudopodia can be found around the cells. The uneven surface of cells under the AFM is due to the villi on them. When the cells were exposed to microwave and Fe_3O_4 for 5 min, we found the number of villi decreased significantly from the SEM image. Moreover, under the AFM, the cells began to shrink and the pseudopodia had noticeably disappeared. These findings suggest that the cells had begun to activate apoptosis. With the continuous stimulation from microwave and Fe_3O_4, noticable pathological changes of A375 cells were found. In the 10 min group, the cells without villi shrunk significantly. Through the AFM, little membrane blebbing appeared around the cells. In the 15 min group, apparent membrane blebbing can be observed in the SEM image, indicating apoptosis had been fully activated. From the AFM, we could also find membrane blebbing appear. With apoptosis fully activated, typical features of apoptosis were found in the 20 min group. From the SEM, we could find the wrinkled cells were covered with membrane blebbing. Moreover, cell fragmentation and apoptotic body were found under the AFM. Different from other cell death pathways, the most characteristic morphological features of apoptosis are membrane blebbing and apoptotic body.[25] In this study, the formation of membrane blebbing as well as the apoptotic body were all captured. Consequently, through the findings from SEM and AFM, we further testified the whole process of cell apoptosis under the stimulation of microwave and Fe_3O_4. We have already investigated the morphological changes of the nucleus, dynamic membrane blebbing and changes of the mitochondrial membrane potential ($\Delta\Psi m$) in different groups. To further explore the type of cell death, SEM and TEM were used to observe A375 cells in different groups. As shown in (Figure 3C), the normal A375 cells are rounded and plump with uniform villi on their surface. As we know, apoptosis is characterized by

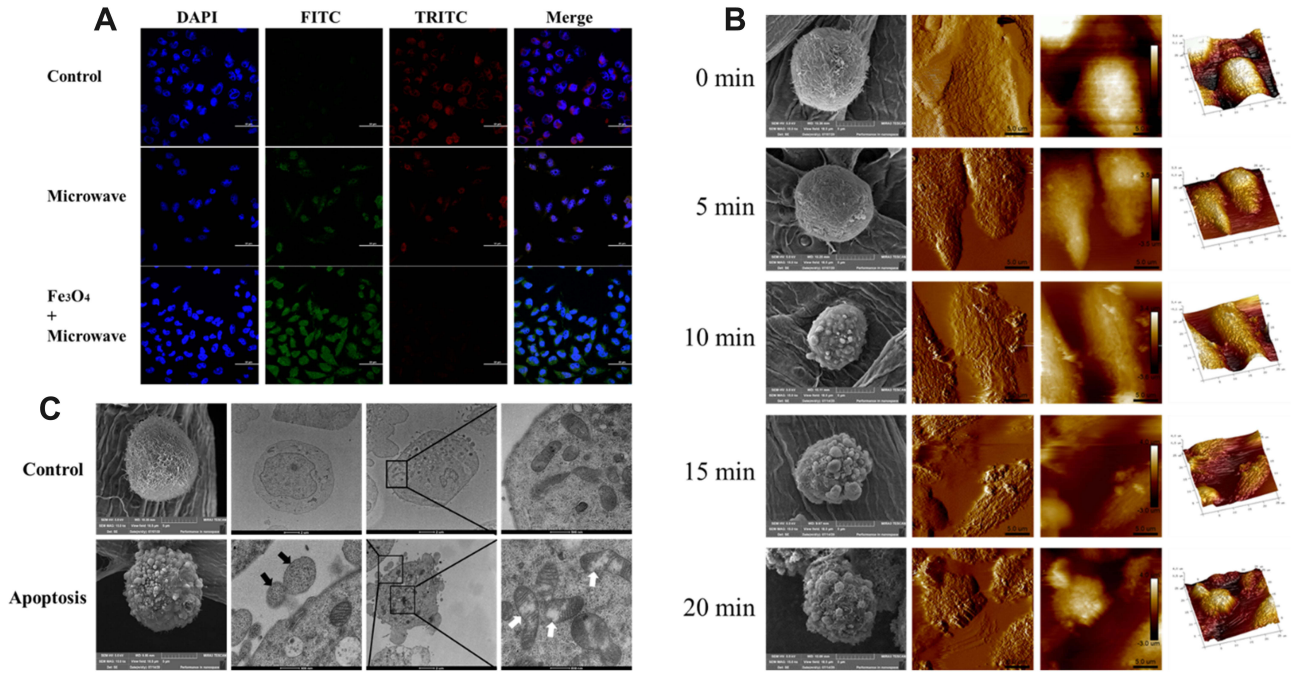

Figure 3 (**A**) Mitochondrial membrane potential (ΔΨm). Red fluorescence (J-aggregates) suggests the high ΔΨm and green fluorescence (J-monomer) suggests the low ΔΨm. The microwave irradiation time is 15 min (2450 MHz, 2W) and the concentration of Fe_3O_4 NPs is 30 μg/mL. (**B**) Dynamic membrane blebbing. The A375 cells were treated with both Fe_3O_4 NPs (30 μg/mL) and mild microwave (2450 MHz, 2W) for different time. (**C**) SEM and TEM images of normal and apoptotic A375 cells. The black arrows indicate apoptotic bodies and the white arrows indicate broken mitochondria.

specific biochemical and morphological changes of dying cells, including nuclear condensation and fragmentation, loss of adhesion to neighbors, dynamic membrane blebbing, and so on.[25,27] As shown in (Figure 3C), membrane blebbing-the most characteristic morphological change of apoptosis-is found in the cells treated with Fe_3O_4 and microwave, indicating the type of cell death is apoptosis. At the same time, compared with the normal A375 cells, the cells treated with Fe_3O_4 and microwave lost their villi and became irregular in shape, which is attributed to the cell apoptosis. As mentioned previously, activation of the IRE1-ASK1-JNK pathway can inhibit anti-apoptotic proteins such as Bcl-2, thus triggering intrinsic apoptosis through damage to mitochondria. In addition, we found that a significant amount of J-monomer had appeared in the microwave and Fe_3O_4 group. As a result, TEM was used to further confirm the occurrence of apoptosis and mitochondria damage. In the control group (Figure 3C), mitochondria with regular morphology and complete structure can be observed in normal A375 cells. In contrast abnormal mitochondria membrane swelling and rupture were observed in cells treated with Fe_3O_4 and microwave. It is obvious that the mitochondrial cristae have disappeared. Meanwhile, apoptotic bodies have appeared around the A375 cells (Figure 3C). The above results further suggest that the cells treated with Fe_3O_4 and microwave underwent apoptosis triggered by ER stress.[29]

In Chen's study, mitochondria-targeting zirconia (ZrO_2) complex nanoparticles (MZCNs) were developed as nanoagents for efficient cancer therapy by microwave ablation. In their study, they found MZCNs induced apparent apoptosis under microwave irradiation. Meanwhile, the direct damage to mitochondria caused by nanoparticles targeting mitochondria is considered to be the main factor for triggering apoptosis.[30] However, based on our findings, severe ER stress caused by nanomaterials and microwave is also crucial in inducing apoptosis.

Microwave Ablation in vivo

Nowadays, antitumor nanomaterials have been widely studied.[31,32] There is a great difference between in vivo and in vitro, for instance, osmotic pressure, pH, inflammatory factors, blood pressure and so on.[33] Consequently, it is important to explore the anti-tumor effect in vivo. To determine the targeting ability of the Fe_3O_4 on melanoma, we tested microwave ablation in mice. B16F10-bearing mice were injected with the Fe_3O_4 via the tail vein, PSB was injected as the control. Then, MRI was used to observe the mice injected with Fe_3O_4 or PBS. In the control group (Figure 4A), the signal intensity of melanoma is slightly higher than that of muscle tissue. However, in the Fe_3O_4 group (Figure 4B), the melanoma

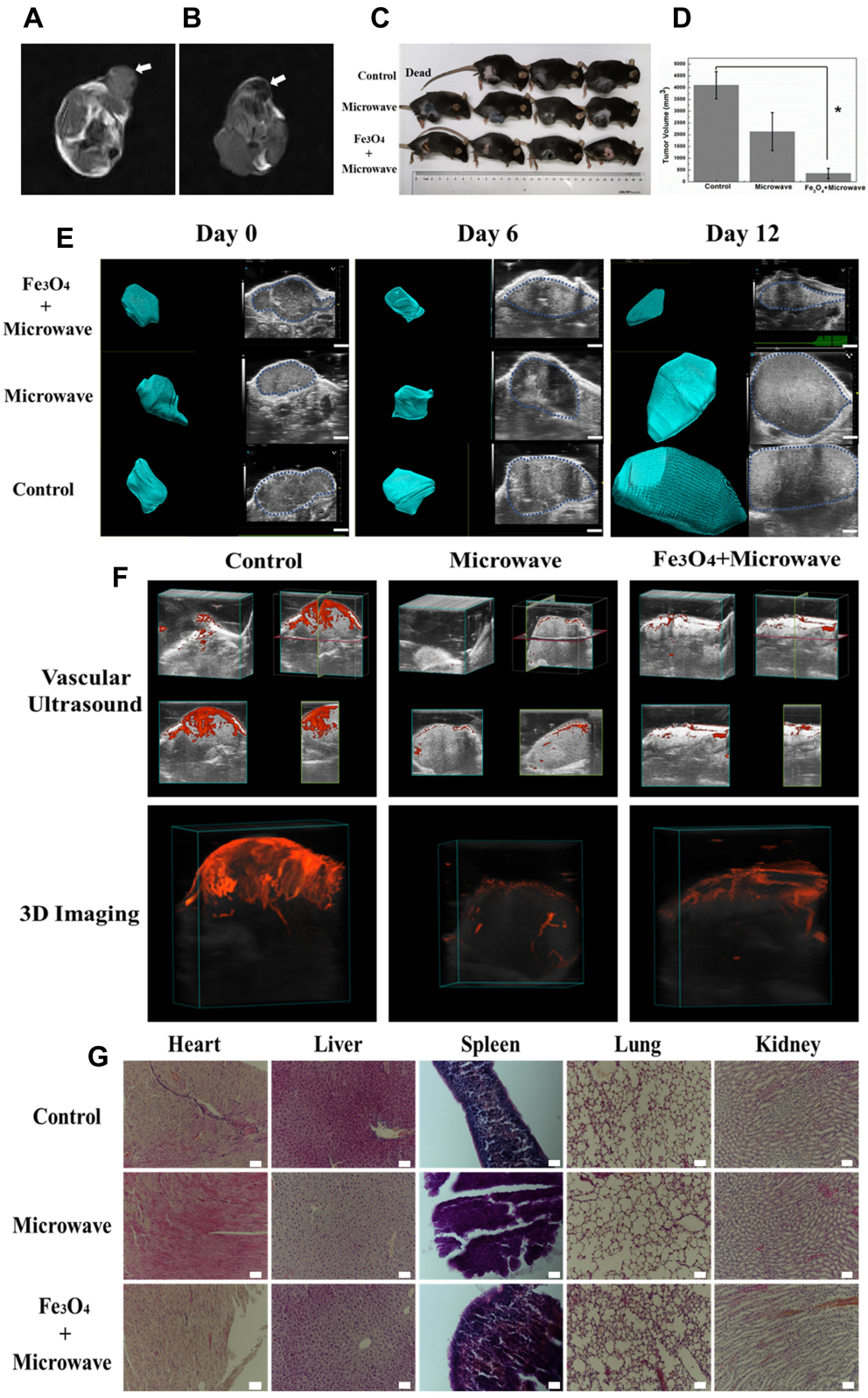

Figure 4 (**A**) MRI of B16F10-bearing mice injected with PBS via the tail vein. White arrow indicates tumor. (**B**) MRI of B16F10-bearing mice injected with Fe_3O_4 NPs (50 mg/Kg) via the tail vein. White arrow indicates tumor. (**C** and **D**) Tumor volume (*$p < 0.05$). (**E**) Ultrasound images of tumor. Injection dose is 50 mg/Kg and the microwave irradiation time is 25 min (2450 MHz, 4W), the scale bar is 2 mm. (**F**) Vascular ultrasound and 3D imaging. (**G**) HE sections of major organs (heart, liver, spleen, lung, kidney) and the bar is 50 μm.

exhibited a significantly lower signal. The low signal suggests that the Fe_3O_4 NPs gathered in the tumor tissue. In this study, a multi-mode ultrasound imaging system was used to monitor the tumor volume and reconstruct the tumor in three dimensions. As shown in Figure 4C–E, the tumor in the control group grew rapidly and had grown to 4102.2 ± 579.5 mm^3 on the 12th day. Such rapid growth may be due to the high malignancy of melanoma.[34] In the microwave group (Figure 4C–E), the growth of melanoma was significantly inhibited, which may be attributed to that continuous microwave stimuli induced ER stress and triggered intrinsic apoptosis. The mean volume of tumor in the Fe_3O_4 + microwave group was 351.6 ± 215.1 mm^3, indicating that melanoma had been inhibited effectively (Figure 4C–E). Based on previous findings, microwave and Fe_3O_4 may induce severe ER stress and terminal UPR, resulting in extensive apoptosis. Owing to the mild microwave, the treatment in this study may cause fewer side effects and have excellent clinical potential. As shown in Figure 4G, the major organs (heart, liver, spleen, lung, kidney) of different groups exhibit no apparent abnormality.

Nutrient supply by blood vessels is essential for the growth of solid tumors.[35,36] In this study, blood vessels of tumors in different groups were observed through a multi-mode ultrasound imaging system. In the control group (Figure 4F), different sections of tumor vessels indicate that melanoma is highly vascular. From the 3D ultrasound imaging rebuilding (Figure 4F), abundant vascular loops and branched vessels were found. This may be attributed to the abnormal levels of growth factors secreted by tumor and stromal cells, which supports the high proliferative rate of cancer cells. However, in the microwave group (Figure 4F), numbers of vessel and vascular loops were reduced significantly. Only one noticeable vessel can be observed in the 3D image. These findings indicate that in addition to inducing ER stress, continuous microwave stimuli may also affect tumor angiogenesis. Clinically, the expression of vascular endothelial growth factor (VEGF) – a most important factor promoting angiogenesis – can be viewed as the prognostic factors of metastasis and recurrence.[37–39] In Wang's study, they found that microwave ablation may achieve a similar clinical effect compared to hepatic resection while not increase the metastasis and recurrence rate.[37] As a result, microwave may inhibit tumor angiogenesis to some extent. Interestingly, in the Fe_3O_4 + microwave group (Figure 4F), only minute blood vessels can be observed. This may be attributed to that Fe_3O_4 enhanced the effect of the microwave. Interestingly, these findings suggest that microwave can not only induce ER stress but also inhibit angiogenesis to some extent. However, the detailed molecular biological mechanism of angiogenesis inhibition induced by microwave needs further research.

Conclusion

In this study, we found that a kind of magnetite Fe_3O_4 nanoparticles could induce severe ER stress and activate cancer apoptosis under mild microwave irradiation. Changes in nuclear and mitochondrial membrane potential, as well as the dynamic membrane blebbing, indicated that apoptosis was triggered. In addition, apparent apoptosis had been observed in the A375 cells under a scanning electron microscope and transmission electron microscope. Moreover, melanoma had also been inhibited effectively in vivo. As a result, the endoplasmic reticulum stress is a promising target with clinical potential in nanomedicine and cancer therapy.

Acknowledgments

This study was funded by the National Natural Science Foundation of China (81472610 and 81672310). We also kindly thank Shanghai Sorrento Medical Technology CO., LTD. for financial and instrument support.

Disclosure

The authors report no conflicts of interest for this work.

References

1. Albukhaty S, Al-Musawi S, Abdul Mahdi S, et al. Investigation of dextran-coated superparamagnetic nanoparticles for targeted vinblastine controlled release, delivery, apoptosis induction, and gene expression in pancreatic cancer cells. *Molecules*. 2020;25(20):4721. doi:10.3390/molecules25204721
2. Long D, Liu TL, Tan LF, et al. Multisynergistic platform for tumor therapy by mild microwave irradiation-activated chemotherapy and enhanced ablation. *ACS Nano*. 2016;10(10):9516–9528. doi:10.1021/acsnano.6b04749
3. Hetz C, Papa FR. The unfolded protein response and cell fate control. *Mol Cell*. 2018;69(2):169–181. doi:10.1016/j.molcel.2017.06.017
4. Hetz C. The unfolded protein response: controlling cell fate decisions under ER stress and beyond. *Nat Rev Mol Cell Biol*. 2012;13(2):89–102. doi:10.1038/nrm3270
5. Iurlaro R, Muñoz-Pinedo C. Cell death induced by endoplasmic reticulum stress. *FEBS J*. 2016;283(14):2640–2652. doi:10.1111/febs.13598
6. Almanza A, Carlesso A, Chintha C, et al. Endoplasmic reticulum stress signalling - from basic mechanisms to clinical applications. *FEBS J*. 2019;286:241–278.
7. Lin Y, Jiang M, Chen W, Zhao T, Wei Y. Cancer and ER stress: mutual crosstalk between autophagy, oxidative stress and inflammatory response. *Biomed Pharmacother*. 2019;118:109249. doi:10.1016/j.biopha.2019.109249

8. Liu J, Sun Z, Deng Y, et al. Highly water-dispersible biocompatible magnetite particles with low cytotoxicity stabilized by citrate groups. *Angew Chem Int Ed Engl*. 2009;48(32):5875–5879. doi:10.1002/anie.200901566
9. Li T, Wu Q, Wang W, et al. MOF-derived nano-popcorns synthesized by sonochemistry as efficient sensitizers for tumor microwave thermal therapy. *Biomaterials*. 2020;234:119773. doi:10.1016/j.biomaterials.2020.119773
10. Fu C, Zhou H, Tan L, et al. Microwave-activated Mn-doped zirconium metal-organic framework nanocubes for highly effective combination of microwave dynamic and thermal therapies against cancer. *ACS Nano*. 2018;12(3):2201–2210. doi:10.1021/acsnano.7b08868
11. Xu J, Cheng X, Tan L, et al. Microwave responsive nanoplatform via P-selectin mediated drug delivery for treatment of hepatocellular carcinoma with distant metastasis. *Nano Lett*. 2019;19(5):2914–2927. doi:10.1021/acs.nanolett.8b05202
12. Li S, Tan L, Xu W, et al. Doxorubicin-loaded layered MoS2 hollow spheres and its photothermo-chemotherapy on hepatocellular carcinoma. *J Biomed Nanotechnol*. 2017;13(11):1557–1564. doi:10.1166/jbn.2017.2461
13. Li S, Yang S, Liu C, et al. Enhanced photothermal-photodynamic therapy by indocyanine green and curcumin-loaded layered mos2 hollow spheres via inhibition of P-glycoprotein. *Int J Nanomedicine*. 2021;16:433–442. doi:10.2147/IJN.S275938
14. Wang M, Law ME, Castellano RK, Law BK. The unfolded protein response as a target for anticancer therapeutics. *Crit Rev Oncol Hematol*. 2018;127:66–79. doi:10.1016/j.critrevonc.2018.05.003
15. Schwarz DS, Blower MD. The endoplasmic reticulum: structure, function and response to cellular signaling. *Cell Mol Life Sci*. 2016;73(1):79–94. doi:10.1007/s00018-015-2052-6
16. Huo L, Chen R, Zhao L, et al. Silver nanoparticles activate endoplasmic reticulum stress signaling pathway in cell and mouse models: the role in toxicity evaluation. *Biomaterials*. 2015;61:307–315. doi:10.1016/j.biomaterials.2015.05.029
17. Yang W, Tiffany-Castiglioni E, Koh HC, Son IH. Paraquat activates the IRE1/ASK1/JNK cascade associated with apoptosis in human neuroblastoma SH-SY5Y cells. *Toxicol Lett*. 2009;191(2–3):203–210. doi:10.1016/j.toxlet.2009.08.024
18. Delbridge AR, Grabow S, Strasser A, Vaux DL. Thirty years of BCL-2: translating cell death discoveries into novel cancer therapies. *Nat Rev Cancer*. 2016;16(2):99–109. doi:10.1038/nrc.2015.17
19. Yang Q, Wang Y, Yang Q, et al. Cuprous oxide nanoparticles trigger ER stress-induced apoptosis by regulating copper trafficking and overcoming resistance to sunitinib therapy in renal cancer. *Biomaterials*. 2017;146:72–85. doi:10.1016/j.biomaterials.2017.09.008
20. Young CN, Cao X, Guruju MR, et al. ER stress in the brain subfornical organ mediates angiotensin-dependent hypertension. *J Clin Invest*. 2012;122(11):3960–3964. doi:10.1172/JCI64583
21. Testerink N, van der Sanden MH, Houweling M, Helms JB, Vaandrager AB. Depletion of phosphatidylcholine affects endoplasmic reticulum morphology and protein traffic at the Golgi complex. *J Lipid Res*. 2009;50(11):2182–2192. doi:10.1194/jlr.M800660-JLR200
22. Wu T, Dai Y. Tumor microenvironment and therapeutic response. *Cancer Lett*. 2017;387:61–68. doi:10.1016/j.canlet.2016.01.043
23. Hui L, Chen Y. Tumor microenvironment: sanctuary of the devil. *Cancer Lett*. 2015;368(1):7–13. doi:10.1016/j.canlet.2015.07.039
24. DeBerardinis RJ, Phimister EG. Tumor microenvironment, metabolism, and immunotherapy. *N Engl J Med*. 2020;382(9):869–871. doi:10.1056/NEJMcibr1914890
25. Van Cruchten S, Van Den Broeck W. Morphological and biochemical aspects of apoptosis, oncosis and necrosis. *Anat Histol Embryol*. 2002;31(4):214–223. doi:10.1046/j.1439-0264.2002.00398.x
26. Ouyang L, Shi Z, Zhao S, et al. Programmed cell death pathways in cancer: a review of apoptosis, autophagy and programmed necrosis. *Cell Prolif*. 2012;45(6):487–498. doi:10.1111/j.1365-2184.2012.00845.x
27. Fleisher TA. Apoptosis. *Ann Allergy Asthma Immunol*. 1997;78(3):245–249. doi:10.1016/S1081-1206(10)63176-6
28. Wang X, Zhang C, Yan X, et al. BH3 mimetic efficiently inhibits colon cancer via cascade effects of mitochondria. *Clin Cancer Res*. 2016;22(6):1445–1458. doi:10.1158/1078-0432.CCR-15-0732
29. Jeong SY, Seol DW. The role of mitochondria in apoptosis. *BMB Rep*. 2008;41(1):11–22. doi:10.5483/BMBRep.2008.41.1.011
30. Chen X, Fu C, Wang Y, Wu Q, Meng X, Xu K. Mitochondria-targeting nanoparticles for enhanced microwave ablation of cancer. *Nanoscale*. 2018;10(33):15677–15685. doi:10.1039/C8NR03927E
31. Ji X, Kong N, Wang J, et al. A novel top-down synthesis of ultrathin 2D boron nanosheets for multimodal imaging-guided cancer therapy. *Adv Mater*. 2018;18(36):e1803031. doi:10.1002/adma.201803031
32. Xing C, Chen S, Qiu M, et al. Conceptually novel black phosphorus/cellulose hydrogels as promising photothermal agents for effective cancer therapy. *Adv Healthc Mater*. 2018;7(7):e1701510. doi:10.1002/adhm.201701510
33. Frankel T, Lanfranca MP, Zou W. The role of tumor microenvironment in cancer immunotherapy. *Adv Exp Med Biol*. 2017;1036:51–64.
34. Spencer KR, Mehnert JM. Mucosal melanoma: epidemiology, biology and treatment. *Cancer Treat Res*. 2016;167:295–320.
35. Viallard C, Larrivée B. Tumor angiogenesis and vascular normalization: alternative therapeutic targets. *Angiogenesis*. 2017;20(4):409–426. doi:10.1007/s10456-017-9562-9
36. Krishna Priya S, Nagare RP, Sneha VS, et al. Tumour angiogenesis-origin of blood vessels. *Int J Cancer*. 2016;139(4):729–735. doi:10.1002/ijc.30067
37. Wang ZL, Liang P, Dong BW, Yu XL, Yu DJ. Prognostic factors and recurrence of small hepatocellular carcinoma after hepatic resection or microwave ablation: a retrospective study. *J Gastrointest Surg*. 2008;12(2):327–337. doi:10.1007/s11605-007-0310-0
38. Apte RS, Chen DS, Ferrara N. VEGF in signaling and disease: beyond discovery and development. *Cell*. 2019;176(6):1248–1264. doi:10.1016/j.cell.2019.01.021
39. Carmeliet P. VEGF as a key mediator of angiogenesis in cancer. *Oncology*. 2005;69(3):4–10. doi:10.1159/000088478